Neuroradiology (2014) 56:129–137
DOI 10.1007/s00234-013-1296-9

INTERVENTIONAL NEURORADIOLOGY

Evaluation of a newly designed flow diverter for the treatment of intracranial aneurysms in an elastase-induced aneurysm model, in New Zealand white rabbits

Andreas Simgen · Desiree Ley · Christian Roth · Umut Yilmaz · Heiko Körner · Ruben Mühl-Benninghaus · Yoo-Jin Kim · Bruno Scheller · Wolfgang Reith

Received: 30 July 2013 / Accepted: 21 October 2013 / Published online: 14 November 2013

Abstract
Introduction In this study, we analyzed angiographic and histologic aneurysm occlusion of a newly designed flow-diverting device. Visibility and flexibility, as well as occlusions of side branches and neointimal proliferation were also evaluated.
Methods Aneurysms were induced in 18 New Zealand white rabbits and treated with a braided, "closed-loop-designed" device of nitinol. Additional devices were implanted in the abdominal aorta to cover the origin of branch arteries. Angiographic follow-ups were performed immediately after placement of the device, after 3 months ($n=9$) and 6 months ($n=9$). The status of aneurysm occlusion (using a five-point scale) and the patency of branch arteries were assessed.
Results Aneurysm occlusion rates were noted as grade 0 in 2 (11 %), grade I in 1 (6 %), grade II in 1 (6 %), grade III in 9 (50 %), and grade IV in 5 (28 %) of 18 aneurysms, respectively, indicating a complete or near-complete occlusion of 78 % under double antiplatelet therapy. Aneurysm occlusion was significantly higher at 6 months follow-up ($P=0.025$). Radiopaque markers provided excellent visibility. Limited device flexibility led to incomplete aneurysm neck coverage and grade 0 occlusion rates in two cases. Distal device occlusions were found in three cases, most likely due to an extremely undersized vessel diameter in the subclavian artery. No case of branch artery occlusion was seen. Intimal proliferation and diameter stenosis were moderate.
Conclusion The tested flow diverter achieved near-complete and complete aneurysm occlusion under double antiplatelet therapy of elastase-induced aneurysms in 78 %, while preserving branch arteries.

Keywords Intracranial aneurysms · Animal model · Flow diverter · Stening

Abbreviations

FD	Flow diverter
DSA	Digital subtraction angiography
AA	Abdominal aorta
SA	Subclavian artery
ICA	Internal carotid artery
PED	Pipeline embolization device
SFD	SILK flow diverter

Introduction

Over the past 20 years, the endovascular treatment of intracranial aneurysms has developed rapidly and become a standard method of treatment. At first the therapy of intracranial

A. Simgen (✉) · D. Ley · U. Yilmaz · H. Körner · R. Mühl-Benninghaus · W. Reith
Department of Neuroradiology, Saarland University Hospital, Kirrberger Str., 66424 Homburg, Germany
e-mail: andreassimgen@googlemail.com

C. Roth
Department of Neuroradiology, Clinic Bremen-Mitte, Bremen, Germany

Y.-J. Kim
Department of Pathology, Saarland University Hospital, Homburg, Saarland, Germany

B. Scheller
Department of Cardiology, Saarland University Hospital, Homburg, Saarland, Germany

aneurysms focused on filling the aneurysm sac with embolic materials. The occlusion of intracranial aneurysms with coil embolization is widely applied and has proven to be a safe method with good occlusion rates [1, 2]. Nevertheless, due to the morphology of particular aneurysms, treatment with coils still holds a risk of incomplete occlusion, leading to different complications such as coil protrusions, further associated with thromboembolic events and recanalization of the aneurysm leading to potential growth or re-rupturing of the aneurysm [3, 4]. The introduction of self-expanding stents led to the concept of treating intracranial aneurysms solely by the use of flow-diverting stent systems. The objective of flow diverters is to treat complex intracranial aneurysms, such as wide-necked, fusiform aneurysms as well as dissecting and giant aneurysms. Nowadays, only a few of these devices have been admitted to the European market although they have shown acceptable safety and efficacy in preclinical and clinical studies [5–9]. The reason is that there are still some notable safety concerns limiting the use of flow diverters (FDs): the potential occlusion of side branches or perforating arteries which carry the risk of secondary ischemic complications, the occurrence of a stent thrombosis leading to an occlusion of the parent vessel, and delayed aneurysm rupture due to intra-aneurysmal thrombosis and the effects of blood flow changes [10–16].

The purpose of our study was to evaluate the in vivo performance of a newly designed FD prototype (manufactured by Admedes Schuessler GmbH, Pforzheim, Germany) without intrasaccular coil placement. We report about angiographic and histologic rates of aneurysm occlusion, patency of branch arteries covered by the device, growth of neointimal layer covering the aneurysm neck, and diameter stenosis of the stented artery segments.

Material and methods

Animal experiment

All the experiments were approved by the animal protection committee of our university and conducted in accordance with the animal experiment guidelines. Elastase-induced aneurysms were created in 18 New Zealand female white rabbits as first described by Kallmes et al. [17]. All the animals received anticoagulation therapy of aspirin (10 mg/kg orally) and clopidogrel (10 mg/kg orally) from 3 days prior to placement of the FD until their sacrifice.

Group 1 ($n=9$) was evaluated over a period of 3 months, a total of 17 FDs were implanted, nine across the necks of the aneurysms and eight in the abdominal aorta. Group 2 ($n=9$) was evaluated over a period of 6 months holding a total of 20 FDs, 9 across the necks of the aneurysms and 11 in the abdominal aorta (AA), resulting in two of the animals having one additional FD implanted in the AA.

Stent design

In comparison to the first FDs like the pipeline embolization device (PED) and the SILK flow diverter (SFD) [5, 9, 18, 19], the applied FD prototype is also a self-expanding stent of 48 braided wires, yet only composed of nitinol, while also incorporating a newly "closed-loop design." The "closed-loop design" signifies that all the wires run in loops from the distal end of the device back to the proximal end of the device, where all the wires are merged and fixated in one radiopaque platinum marker. The purpose of the stent design is to provide atraumatic placement and prevent loose wires from irritating the vessel wall. For better visibility, the stent also holds four radiopaque platinum markers on its distal end and only one radiopaque marker on its proximal end. Since all the wires merge in the proximal radiopaque marker, the device shows proximally an oval, sloping running end (Fig. 1). The wires themselves have different calibers, of which 44 measure 35 μm and 4 measure 85 μm, while the PED and the SFD have wires of the same size with a diameter of approximately 35 μm. The closed loops and different wire calibers improve the expansion of the stent and its apposition to the vessel wall due to its high radial force. The utilized devices had a nominal diameter of 4.5 mm and were available at a length of 20–40 mm. A braiding angle of 55° leads to a relative consistent pore size, foreshortening, and porosity at different vessel diameters of the 4.5 mm device used (Table 1). When expanded to its nominal diameter, the device provides less metal coverage, 20–25 %, in comparison to the PED (30–35 %) and SFD (35–55 %). The proximal marker is connected to a transport wire and was preloaded into an introducer. Placement of the FD can be accomplished with a standard microcatheter with an inner diameter of 0.025 in. and an outer diameter of 3 French.

Stent placement

In general anesthesia and under sterile conditions, the right femoral artery was surgically exposed, and a 3-French vascular sheath was inserted in a retrograde manner. A 3-French

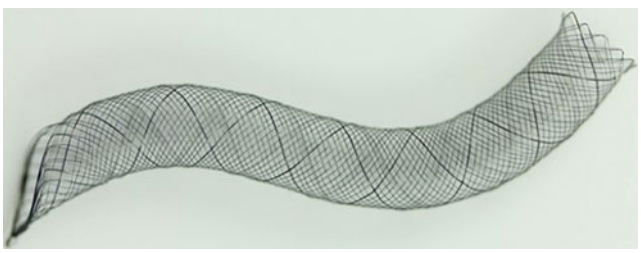

Fig. 1 Photograph of the closed-loop design prototype FD (manufactured by Admedes Schuessler GmbH, Pforzheim, Germany). Distally, all the wires run in loops leading back to the proximal end of the device where all wires merge in one radiopaque marker

Table 1 Technical details of the FD with a nominal diameter of 4.5 mm

Vessel diameter	3 mm	4 mm
Pore size	0.302 mm	0.346 mm
Porosity	78.2 %	80.8 %
Foreshortening	16 %	30 %

hydrophilic microcatheter was then introduced to the sheath and throughout the procedure flushed with a heparinized saline. The animals received 300 U of heparin intravenously. Under radioscopic guidance, the microcatheter was placed in the brachiocephalic trunk and digital subtraction angiography (DSA) was performed to evaluate the aneurysm. After establishing a roadmap angiogram, the microcatheter was placed in the subclavian artery distal to the aneurysm using a microguidewire (Silverspeed 0.010 inch; Covidien/eV3). The wire was removed and the preloaded flow diverter introduced to the microcatheter. Deployment was executed across the neck of the aneurysm by slowly pushing the transport wire while gently retrieving the microcatheter at the same time. As soon as the FD was pushed out of the microcatheter, distal opening of the device was visible due to the four distal markers. Retraction of the FD back into the microcatheter was achievable as long as the distal marker of the microcatheter was distal to the proximal stent marker. Because of the closed-loop design and its sloping, oval proximal running end, the FD had to be deployed with an overlap of 10 mm proximal to the aneurysm neck in order to ensure full coverage of the aneurysm. After removing the transport wire, DSA series were performed to assess the flow pattern of the contrast media in the aneurysm. The microcatheter was then placed in the abdominal aorta and an additional FD was deployed using a roadmap angiogram to ensure the coverage of lumbar and renal arteries. Subsequently, DSA series were performed to ensure patency of the covered arteries. In two animals we implanted two FDs in the AA immediately one after another across the origin of both renal arteries and lumbar arteries.

All endovascular materials were then removed, the femoral artery ligated, and the wound was sewn. Anticoagulation therapy was continued until sacrifice of the animals.

Angiographic follow-up and sacrifice of the animals

The animals were followed up after 3 months ($n=9$) and after 6 months ($n=9$) immediately prior to their sacrifice. In general anesthesia and under sterile conditions, the left carotid artery was surgically exposed. After introducing a 4-French sheath to the vessel in a retrograde manner, DSA series were performed. Then, the animals were sacrificed with a lethal injection of pentobarbital. After extracting the aneurysms and parts of the AA, the specimens were fixed in a 10 % solution of phosphate-buffered formaldehyde.

Histological processing

The formalin-fixed stented artery segments were immersed in methylmethacrylate. Representative cross sections of the stents were cut from the block, polished, and glued on acrylic plastic slides [20]. The final specimens were then stained with hematoxylin–eosin (H&E). From the artery segment, including the aneurysm, sectional slices were cut from the block while additional slices were prepared distally. From the aortic stented segment, axial sections were taken from the midportion of the stent and another one from the distribution of branch arteries. After microscopy (Eclipse 80i; Nikon, Düsseldorf, Germany) and digitization, an experienced neuropathologist conducted histopathological evaluations. The parameters evaluated were thrombus formation in the aneurysm sac, neointimal spreading along the aneurysm neck, neointimal thickness, diameter stenosis, the patency of abdominal branch arteries, and inflammation surrounding the stent struts.

Morphometric measurements were performed as follows: Thickness of the neointima = distance between the outer surface of each strut and the luminal border. Neolumen = distance from luminal border to luminal border. Former vessel lumen = distance from the outside of a strut to the opposite outside of the strut across the vessel diameter. Diameter stenosis = (neolumen÷former lumen)×100.

Statistical analysis

All the statistical evaluations were conducted with SPSS software (SPSS, Inc., Chicago, IL). Average data is presented as mean±standard deviation. The chi^2 test was also applied to determine differences in frequencies. Differences in means were tested using Student's t tests.

Results

Angiographic evaluation

Two observers, in consensus, analyzed angiograms using a five-point grading scheme for the occlusion of saccular aneurysms as described in literature [21] as the following: grade 0, no endoaneurysmal flow changes; grade I, residual filling >50 %; grade II, residual filling <50 %; grade III, near complete occlusion with residual filling at the aneurysm neck; grade IV, complete occlusion. Aneurysm sizes are shown in Table 2.

Table 2 Aneurysm sizes in the different groups represented as mean±SD

Time, months	Neck, mm	Width, mm	Height, mm
3	2.7±0.6	2.6±0.8	5.4±1.2
6	2.6±0.7	2.8±0.9	5.6±1.7
P value	0.925	0.617	0.806

In all cases, the delivery and deployment of the devices were successful. In three cases, we experienced only a partial opening of the distal end of the device due to a vessel diameter of less than 3 mm (distal subclavian artery), leading to delayed stent occlusion. Due to the distal radiopaque markers, partial opening of the three devices was apparent during the process of delivery. The thicker wires of 85 μm did not improve the visibility of the device since these, as well as the mesh system, could not be seen under fluoroscopy after implantation (Figs. 2 and 3). Stent design allowed the device to be retracted into the microcatheter after near complete deployment of around 95 %. Therefore, it was possible to reposition the device at any time during the procedure. We observed limited flexibility of the device, which made delivery challenging in eight cases, in which the subclavian artery showed a tortuous course (Fig. 4). In such settings, straightening of the subclavian artery (Fig. 4) was seen and, in combination with proximity to the pulsating heart, it led to difficulties in the exact placement of the device. Because of the proximal stent design (oval sloped running end), the device had to be deployed with a proximal overlap of 10 mm to ensure full coverage of the aneurysm neck. In two of these eight cases, measurements of the distance between the aneurysm and the proximal marker of the device revealed a deployment of less than 10 mm so marginal deployment concerning the overlapping of the aneurysm neck had to be assumed. DSA immediately following deployment of the FD showed a faster washout of the contrast medium within the aneurysm; however, as in all other cases, secure stasis of contrast medium was observed due to a reduced outflow of the aneurysm after deployment of the FD (Fig. 5). No cases of immediate aneurysm occlusion after stent placement were seen.

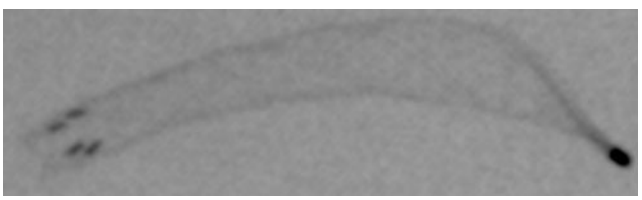

Fig. 2 Fluoroscopy of the prototype FD not implanted in an animal. The five platinum radiopaque markers are clearly visible. The thicker wires measuring 85 μm are made of nitinol and the mesh system itself is slightly definable

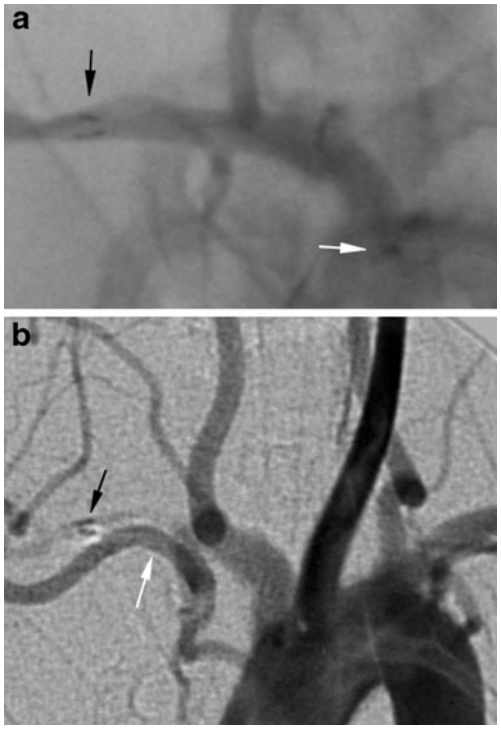

Fig. 3 **a** Fluoroscopy after implantation of the FD showing partial opening of the distal device visible due to the radiopaque markers (*black arrow*). The *white arrow* shows the proximal marker of the device. **b** DSA of the occluded FD (*black arrow*) after 6 months demonstrating good vessel collateralization (*white arrow*) and a complete aneurysm occlusion grade IV

Taking into consideration the anticoagulation therapy administered throughout the entire period of observation, overall occlusion rates of grades 0, I, II, III, and IV were noted in 2 (11 %), 1 (6 %), 1 (6 %), 9 (50 %), and 5 (28 %) of 18 aneurysms, respectively.

At 3 months, grades 0, I, II, and III occlusion rates were noted in two (22 %), one (11 %), one (11 %), and five (56 %) of nine aneurysms, respectively, while no complete aneurysm occlusion was observed. In five cases, most of the aneurysm lumen was occluded with a small remnant, reducing flow at the aneurysm neck (Fig. 5). In two cases, the aneurysms angiographically showed no occlusion but histology afterwards proved unsuccessful positioning of the FD, leading to incomplete coverage of the aneurysm neck by the FD.

At 6 months, only grade III and IV occlusion rates were noted in four (44 %) and five (56 %) of nine aneurysms ($P=0.025$), respectively. In four cases, small remnants were seen at the necks of the aneurysms.

All branch arteries covered by the FDs, such as vertebral, renal, and lumbar arteries, remained patent at each follow-up (Fig. 6). The mean diameter of these branch vessels was measured as follows: vertebral artery 1.6±0.3 mm, lumbar artery 1.2±0.2 mm, and renal artery 2.1±0.5 mm.

In three cases (two at 3-month follow-up and one at 6-month follow-up), the FD was deployed very distally in the

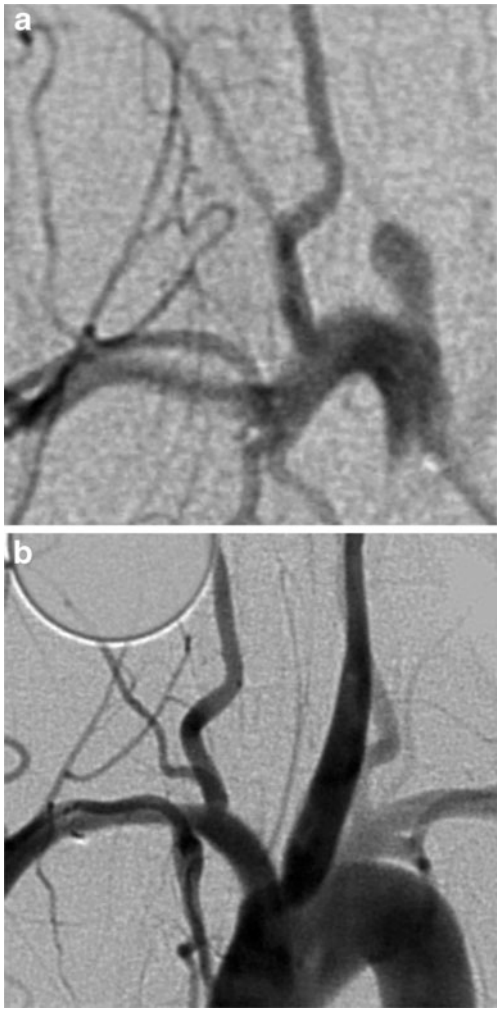

Fig. 4 **a** Extreme tortuosity of the subclavian artery. **b** DSA follow-up at 6 months shows straightening of the subclavian artery after FD implantation and a completely occluded aneurysm (grade IV)

subclavian artery, reaching a vessel diameter of 2.2±0.3 mm. In the setting of an undersized vessel diameter, the distal end of the device adjusted to the vessel diameter and showed only partial opening. Even though these devices were patent in the DSA immediately after placement, all of them were occluded in the follow-up angiography. Due to the presence of adequate collaterals, the animals showed no neurological deficits and occlusion of the aneurysm was still in progress showing one grade I occlusion after 3 months and one completely occluded aneurysm (grade IV) after 6 months (Fig. 3). The third aneurysm showed no occlusion at all (grade 0) and was one of the two animals with incomplete aneurysm neck coverage.

Histopathological evaluation

After 3-month follow-up, five aneurysms showed partially organized thrombus formation occupying the dome of the aneurysms with a section at the neck showing absent tissue and residual filling with fresh blood (Fig. 7). Two aneurysms were incompletely obliterated with poorly organized thrombus, partially filling the aneurysm dome. In two cases, no aneurysm occlusion was visible in the angiographic follow-up. The sections taken from these two aneurysms showed incomplete coverage of the aneurysm neck by the stent struts, with evidence of fresh blood in the inferior part of the aneurysm. Despite the incomplete coverage in both cases, a partially organized thrombus was seen in the fundus of the aneurysms, as aneurysm embolization was still in progress (Fig. 7). Intimal hyperplasia was thick in one case (>175 μm) and thin in eight cases (<175 μm). In seven aneurysms, neointima was only partially covering the struts across the aneurysm neck. In the two cases with incomplete neck coverage, we observed a neointima throughout the covering struts (Fig. 7). Metaplastic bone formations after 3 months were only seen in the distal segment of the subclavian artery in three cases.

After 6-month follow-up, we observed fibrous connective tissue in four of nine aneurysms filling the aneurysm dome, intermingled with abundant hemosiderin deposits. The other five aneurysms showed partially organized thrombus occupying most of the dome. In four cases, the aneurysm necks were completely covered by neointima, the other five aneurysms only showed incomplete coverage of the stent struts. Intimal

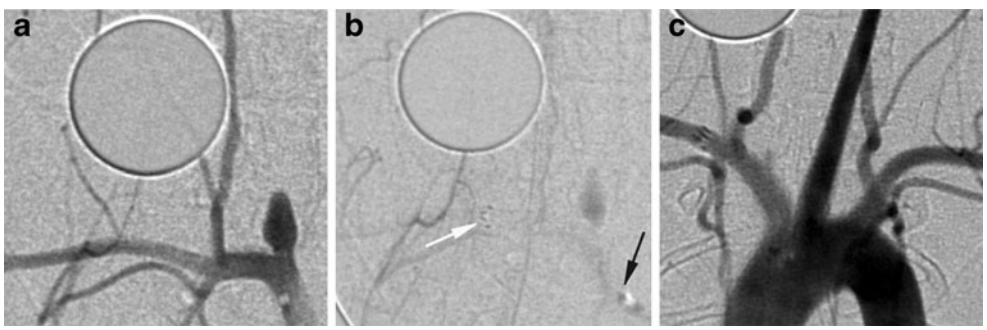

Fig. 5 **a** DSA shows the created aneurysm at the brachiocephalic trunk. **b** DSA immediately after deployment of the FD, with its radiopaque distal markers (*white arrow*) and the proximal marker (*black arrow*), impaired in its visibility due to the pulsation of the heart. Observed stasis of contrast medium within the aneurysm. **c** DSA follow-up after 3 months shows that the aneurysm is nearly occluded with a small remnant at the neck of the aneurysm

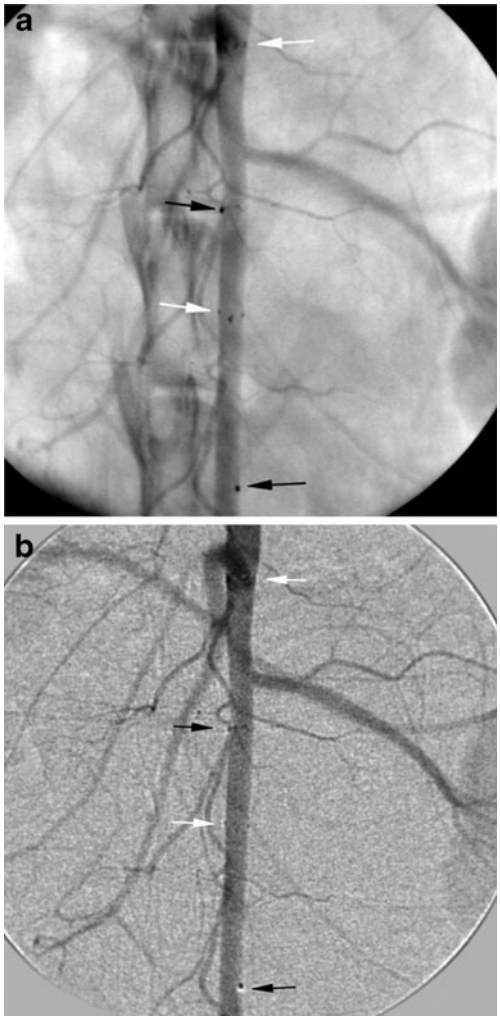

Fig. 6 **a** Fluoroscopy and **b** DSA of the abdominal aorta with two implanted FDs covering both renal arteries and two lumbar arteries, showing patency after 6 months. The *white arrows* indicate the proximal radiopaque markers and the *black arrows* indicate the distal markers of the FDs

hyperplasia was thick in two cases (>175 μm) and thin in all the other cases. Osseous tissue after 6 months was seen in the distal segment of the subclavian artery in four cases, as well as in the segment hosting the aneurysm in two cases.

No evidence of inflammatory response to the stent struts was observed.

Neointimal thickness and diameter stenosis between the subclavian artery and the abdominal aorta was significantly different ($P<0.001$) in both groups, demonstrating a neointima and diameter stenosis in the subclavian artery double the size of that seen in the abdominal aorta after 3 and 6 months (Table 3). The appearance of a thicker neointima in the subclavian artery is more likely to correlate with the proximity of the devices to the aortic arch, resulting in higher mechanical exposure due to the continuous pulsation of the beating heart, than with the devices in the abdominal aorta. Neointimal thickness and diameter stenosis after 3 and 6 months was statistically not significantly different but showed a decreasing tendency after 6 months (Table 3). Furthermore, the neointima covering the origin of branch vessels seemed to be discontinuous (Fig. 7).

Discussion

Most experiences in the field of flow diversion have been gathered using devices with a narrow-mesh system like PED (Covidien/eV3, Irvine, CA) and SFD (Balt, Montmorency, France).

In this study, we report about the evaluation of a newly designed flow diverter prototype aiming at the occlusion of saccular aneurysms. The difference regarding the utilized prototype FD in comparison to the PED and SFD is its complete composition of nitinol—only the radiopaque markers are made of platinum—and the combination of a closed-loop design with different sizes of wires (35 and 85 μm). The prototype also provides less surface coverage of around 20–25 % and a higher porosity of approximately 80 % compared to the PED and SFD. A small angle of twist

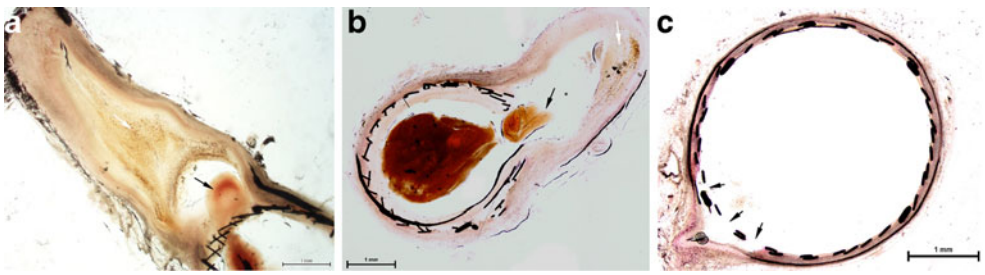

Fig. 7 **a** An aneurysm after 3 months holding fibrous connective tissue in the dome with residues of organized blood (hemosiderin = *white arrow*) and missing tissue at the aneurysm neck with fresh blood (*black arrow*). **b** A non-occluded aneurysm with incomplete coverage of the aneurysm neck by the struts with fresh blood within the parent vessel and at the junction of the aneurysm (*black arrow*). Thick neointimal proliferation of 225 μm (*black line*) covering the entire device, leading to a diameter stenosis of 20 %. The *white arrow* demonstrates a small, organized thrombus formation in the fundus of the aneurysm. **c** Photomicrograph of the stented abdominal aorta after 6 months showing patency of the covered lumbar artery with discontinuous neointima along the struts and thin neointimal proliferation. (H&E original magnification ×20)

Table 3 Morphometric measurements represented as mean±SD

Time, months	Neointimal thickness, μm			Diameter stenosis, %		
	Distal SA	Aneurysm	AA	Distal SA	Aneurysm	AA
3	138±20	146±33	76±17	11±4	13±4	6±1
6	131±31	133±32	66±17	10±4	10±5	4±2
P value	0.619	0.459	0.270	0.549	0.330	0.085

(55°) leads to a stable foreshortening of approximately 30 % at a vessel diameter of 4 mm. Using this prototype FD, we achieved a near-complete (grade III) and complete aneurysm (grade IV) occlusion of 78 %, taking into consideration double antiplatelet therapy with aspirin and clopidogrel throughout the entire period of observation. Therefore, we assume that the occlusion rates achieved in this study can keep up with occlusion rates of similar devices, since antiplatelet therapy in these preclinical studies was discontinued after 10 and 30 days [5, 9].

In the field of flow diversion, the optimal compromise between flexibility, visibility, and efficient flow diverting effect plays an important role. Authors reported that a porosity threshold of about 70 % seems to be a good compromise [9, 22]. In our study, we experienced good visibility of the FD due to radiopaque markers at both ends of the device, the mesh system itself was not visible. Especially the distal markers were very helpful in judging the distal opening of the device during the process of delivery. Another advantage during delivery was the retractability of the device back into the microcatheter after near-complete expansion of around 95 %. This was easily achievable as long as the distal marker of the microcatheter was distal to the proximal device marker. The main disadvantage observed was the limited device flexibility, making delivery in tortuous vessels challenging, which in combination with the proximal oval, sloped running end led to incomplete aneurysm neck coverage in two cases. Although the proximal marker of the device was detached proximally of the aneurysm neck, only partial coverage of the neck could be achieved since the overlap of the devices in these cases was less than 10 mm. The limited flexibility of the device was more likely attributable to its closed-loop design merging all wires in one proximal radiopaque marker and the different wire sizes, of which four measured 85 μm. Since these wires did not help to improve visibility, they had an adverse impact on the flexibility of the device. In comparison to the PED and SILK, the higher porosity of about 80 % perhaps also contributed to the limited flexibility of the device.

Nonetheless, spontaneous distal opening of the device was seen in all 37 cases as soon as the FD was pushed out of the microcatheter. Since only 4.5 mm devices were available and the subclavian artery in rabbits decreases in diameter during its course, devices were relatively oversized in the distal segment of the vessel. Therefore in extreme cases of vessel undersizing (<3 mm), the device only partially opened its distal end, leading to a distal occlusion.

When using flow-diverting devices, concerns about the occlusion of small perforating arteries are still present since several clinical reports that have been published support these findings [23, 24]. Many studies before have shown that the abdominal aorta in rabbits is suitable for the evaluation of branch artery patency [5, 8, 25]. Preclinical studies showed that small branch arteries remain patent even after placement of several overlapping FDs [25]. Since the smallest vessels covered by the device in our study were lumbar arteries with a diameter of 1.2±0.2 mm, we cannot ensure patency of branch or perforating arteries smaller in size. In our study, we experienced no occlusion of side branches covered by the devices.

Neointimal thickness and diameter stenosis was significantly higher in the subclavian artery than in the abdominal aorta at both points in time. The size of the neointima was comparable to those described in other preclinical studies and remained moderate overall [5, 8, 25]. Previous publications described a degression in the neointimal thickness as time passes [8, 26]. Our findings between the neoinitimal thickness and diameter stenosis after 3 and 6 months were statistically not significantly different but showed a decreasing tendency after 6 months.

Like other publications, we also experienced the occurrence of bone formations around the device in some cases. This osseous metaplasia was seen especially in the distal segment of the subclavian artery. Since these findings have been reported in experimental aneurysms after coil treatment [27] and after treatment with flow diverter [5, 8, 25], the relevance remains unclear.

Our major concern about the design of the FD was its limited flexibility, more likely due to the closed-loop design with different size of wires and high porosity, making delivery through tortuous vessels challenging and leading to incomplete coverage of the aneurysm neck. We doubt that the device is flexible enough to meet human requirements, in navigating through the intracranial internal carotid artery and simultaneously ensuring safe treatment of aneurysms. Despite the incomplete aneurysm coverage, the process of aneurysm occlusion was still advancing as histology showed organized thrombus in the fundus of the aneurysms.

Our experiment has several limitations. First, we did not include an untreated aneurysm group, since experience with

this animal model at our department has proven patency of untreated aneurysms. Second, the created aneurysm sizes and morphologies can only be compared to small wide-necked aneurysms so the behavior of giant aneurysms treated with this device remains uncertain. Third, since the vessel anatomy of rabbits cannot be compared with that of humans, trackability of this device in the setting of the human ICA remains uncertain. Finally, we cannot assure the patency of branch arteries smaller than the lumbar arteries in rabbits.

Nonetheless, our study only describes the evaluation of a prototype device. Essential improvements in design have been achieved from the collected information in this study, leading to higher occlusion rates and better flexibility in ongoing experiments (unpublished data).

Conclusion

The tested device showed that occlusion of elastase-induced aneurysms by flow diversion alone can only be achieved after a certain time with excellent patency of small branch arteries. The achieved occlusion rates were promising, considering double antiplatelet therapy throughout the entire period of observation. Due to radiopaque markers, the device showed very good visibility during the process of delivery and in the follow-up angiographies. Interesting results involving stent design, concerning limited flexibility, occurrence of distal device occlusions, and incomplete aneurysm neck coverage have been gathered and will help to improve the development of future flow-diverting devices.

Acknowledgments We would like to thank Admedes Schuessler GmbH, Pforzheim, Germany, for providing the prototype FDs and delivery systems. We would also like to thank the Head of the Department of Experimental Surgery, Prof. Menger, and his team, for supporting this study.

Conflict of interest We declare that we have no conflict of interest.

References

1. Molyneux AJ, Kerr RSC, Yu L-M et al (2005) International subarachnoid aneurysm trial (ISAT) of neurosurgical clipping versus endovascular coiling in 2143 patients with ruptured intracranial aneurysms: a randomised comparison of effects on survival, dependency, seizures, rebleeding, subgroups, and aneurysm occlusion. Lancet 366:809–817
2. McDougall CG, Spetzler RF, Zabramski JM et al (2012) The Barrow Ruptured Aneurysm Trial. J Neurosurg 116:135–144
3. Grunwald IQ, Papanagiotou P, Struffert T et al (2007) Recanalization after endovascular treatment of intracerebral aneurysms. Neuroradiology 49:41–47
4. Gallas S, Januel AC, Pasco A et al (2009) Long-term follow-up of 1036 cerebral aneurysms treated by bare coils: a multicentric cohort treated between 1998 and 2003. AJNR Am J Neuroradiol 30:1986–1992
5. Kallmes DF, Ding YH, Dai D et al (2007) A new endoluminal, flow-disrupting device for treatment of saccular aneurysms. Stroke 38:2346–2352
6. Fiorella D, Woo HH, Albuquerque FC, Nelson PK (2008) Definitive reconstruction of circumferential, fusiform intracranial aneurysms with the pipeline embolization device. Neurosurgery 62:1115–1120
7. Lylyk P, Miranda C, Ceratto R et al (2009) Curative endovascular reconstruction of cerebral aneurysms with the pipeline embolization device: the Buenos Aires experience. Neurosurgery 64:632–642
8. Kallmes DF, Ding YH, Dai D et al (2009) A second-generation, endoluminal, flow-disrupting device for treatment of saccular aneurysms. AJNR Am J Neuroradiol 30:1153–1158
9. Sadasivan C, Cesar L, Seong J et al (2009) An original flow diversion device for the treatment of intracranial aneurysms: evaluation in the rabbit elastase-induced model. Stroke 40:952–958
10. Kulcsar Z, Houdart E, Bonafé A et al (2011) Intra-aneurysmal thrombosis as a possible cause of delayed aneurysm rupture after flow-diversion treatment. AJNR Am J Neuroradiol 32:20–25
11. Turowski B, Macht S, Kulcsár Z et al (2011) Early fatal hemorrhage after endovascular cerebral aneurysm treatment with a flow diverter (SILK-Stent): do we need to rethink our concepts? Neuroradiology 53:37–41
12. Cebral JR, Mut F, Raschi M et al (2011) Aneurysm rupture following treatment with flow-diverting stents: computational hemodynamics analysis of treatment. AJNR Am J Neuroradiol 32:27–33
13. Berge J, Biondi A, Machi P et al (2012) Flow-diverter silk stent for the treatment of intracranial aneurysms: 1-year follow-up in a multicenter study. Am J Neuroradiol 33:1150–1155
14. Fischer S, Vajda Z, Aguilar Perez M et al (2012) Pipeline embolization device (PED) for neurovascular reconstruction: initial experience in the treatment of 101 intracranial aneurysms and dissections. Neuroradiology 54:369–382
15. Maimon S, Gonen L, Nossek E et al (2012) Treatment of intracranial aneurysms with the SILK flow diverter: 2 years' experience with 28 patients at a single center. Acta Neurochir 154:979–987
16. Becske T, Kallmes DF, Saatci I et al (2013) Pipeline for uncoilable or failed aneurysms: results from a multicenter clinical trial. Radiology 267:858–868
17. Cloft HJ, Altes TA, Marx WF et al (1999) Endovascular creation of an in vivo bifurcation aneurysm model in rabbits. Radiology 213:223–228
18. Aurboonyawat T, Blanc R, Schmidt P et al (2011) An in vitro study of silk stent morphology. Neuroradiology 53:659–667
19. Gross BA, Frerichs KU (2013) Stent usage in the treatment of intracranial aneurysms: past, present and future. J Neurol Neurosurg Psychiatry 84:244–253
20. Cremers B, Kelsch B, Clever YP et al (2012) Inhibition of neointimal proliferation after bare metal stent implantation with low-pressure drug delivery using a paclitaxel-coated balloon in porcine coronary arteries. Clin Res Cardiol 101:385–391
21. Kamran M, Yarnold J, Grunwald IQ, Byrne JV (2011) Assessment of angiographic outcomes after flow diversion treatment of intracranial aneurysms: a new grading schema. Neuroradiology 53:501–508
22. Seong J, Wakhloo AK, Lieber BB (2007) In vitro evaluation of flow divertors in an elastase-induced saccular aneurysm model in rabbit. J Biomech Eng 129:863–872
23. Kulcsár Z, Ernemann U, Wetzel SG et al (2010) High-profile flow diverter (Silk) implantation in the basilar artery. Stroke 41:1690–1696

24. van Rooij WJ, Sluzewski M (2010) Perforator infarction after placement of a pipeline flow-diverting stent for an unruptured A1 aneurysm. AJNR Am J Neuroradiol 31:E43–44
25. Dai D, Ding YH, Kadirvel R et al (2012) Patency of branches after coverage with multiple telescoping flow-diverter devices: an in vivo study in rabbits. AJNR Am J Neuroradiol 33:171–174
26. Asakura M, Ueda Y, Nanto S et al (1998) Remodeling of in-stent neointima, which became thinner and transparent over 3 years: serial angiographic and angioscopic follow-up. Circulation 97:2003–2006
27. Dai D, Ding YH, Kadirvel R et al (2007) Bone formation in elastase-induced rabbit aneurysms embolized with platinum coils: report of 2 cases. AJNR Am J Neuroradiol 28:1176–1178